Current Biology

Report

Dense reconstruction of elephant trunk musculature

Graphical abstract

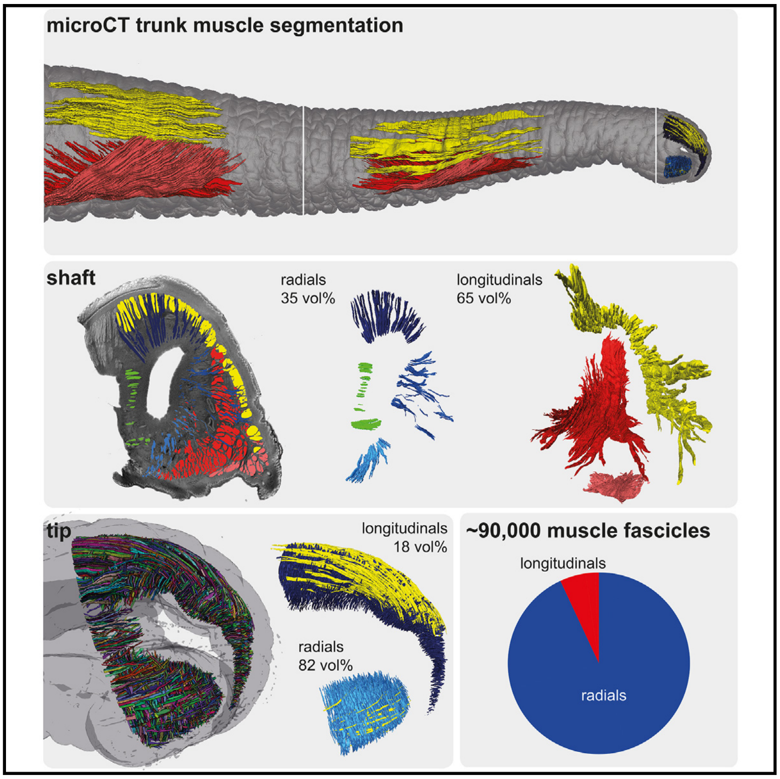

Highlights

- A baby elephant trunk was segmented into muscle fascicles
- Muscle fascicles of the trunk finger are miniaturized
- Radial muscle fascicles dominate the dexterous trunk tip
- An elephant trunk contains ca. 90,000 muscle fascicles

Authors

Luke L. Longren, Lennart Eigen, Ani Shubitidze, ..., John A. Nyakatura, Thomas Hildebrandt, Michael Brecht

Correspondence

michael.brecht@bccn-berlin.de

In brief

Longren et al. applied microCT to the trunk of an Asian baby elephant and show that trunk musculature breaks down into ∼90,000 muscle fascicles. Muscle segmentation suggests that elephant dexterity emerges from muscle number and muscle miniaturization rather than from fine control of individual muscles as is the case in primates.

Longren et al., 2023, Current Biology *33*, 4713–4720
November 6, 2023
https://doi.org/10.1016/j.cub.2023.09.007

Current Biology

CellPress
OPEN ACCESS

Report

Dense reconstruction of elephant trunk musculature

Luke L. Longren,[1,2,8] Lennart Eigen,[1,8] Ani Shubitidze,[1] Oliver Lieschnegg,[1] Daniel Baum,[3] John A. Nyakatura,[4] Thomas Hildebrandt,[5,7] and Michael Brecht[1,6,7,9,10,*]

[1]Bernstein Center for Computational Neuroscience Berlin, Humboldt-Universität zu Berlin, Philippstr. 13, Haus 6, 10115 Berlin, Germany
[2]Technische Universität Berlin, Straße des 17. Juni 135, 10623 Berlin, Germany
[3]Zuse-Institut Berlin, Takustraße 7, 14195 Berlin, Germany
[4]Institut für Biologie, Humboldt-Universität zu Berlin, 10115 Berlin, Germany
[5]Leibniz Institute for Zoo and Wildlife Research, Alfred-Kowalke-Str. 17, 10315 Berlin, Germany
[6]NeuroCure Cluster of Excellence, Humboldt-Universität zu Berlin, 10115 Berlin, Germany
[7]Senior author
[8]These authors contributed equally
[9]X (formerly Twitter): @bccn-berlin
[10]Lead contact
*Correspondence: michael.brecht@bccn-berlin.de
https://doi.org/10.1016/j.cub.2023.09.007

SUMMARY

The elephant trunk operates as a muscular hydrostat[1,2] and is actuated by the most complex musculature known in animals.[3,4] Because the number of trunk muscles is unclear,[5] we performed dense reconstructions of trunk muscle fascicles, elementary muscle units, from microCT scans of an Asian baby elephant trunk. Muscle architecture changes markedly across the trunk. Trunk tip and finger consist of about 8,000 extraordinarily filigree fascicles. The dexterous finger consists exclusively of microscopic radial fascicles pointing to a role of muscle miniaturization in elephant dexterity. Radial fascicles also predominate (at 82% volume) the remainder of the trunk tip, and we wonder if radial muscle fascicles are of particular significance for fine motor control of the dexterous trunk tip. By volume, trunk-shaft muscles[6] comprise one-third of the numerous, small radial muscle fascicles; two-thirds of the three subtypes of large longitudinal fascicles (dorsal longitudinals, ventral outer obliques, and ventral inner obliques);[7–9] and a small fraction of transversal fascicles. Shaft musculature is laterally, but not radially, symmetric. A predominance of dorsal over ventral radial muscles and of ventral over dorsal longitudinal muscles may result in a larger ability of the shaft to extend dorsally than ventrally[10] and to bend inward rather than outward. There are around 90,000 trunk muscle fascicles. While primate hand control is based on fine control of contraction by the convergence of many motor neurons on a small set of relatively large muscles, evolution of elephant grasping has led to thousands of microscopic fascicles, which probably outnumber facial motor neurons.

RESULTS AND DISCUSSION

Without sufficient muscular subdivision, the trunk would lack the physical ability for fine-grained movement. The quantification of trunk muscle number has therefore been a key research question. Classic studies[3] relied on sectioning the trunk and identifying muscles in and across sections,[6] but such approaches led to diverging muscle number estimates[5] (Figure S1). Recent work divided trunk muscles into functional zones.[11] Our approach centered on identifying, tracing, and quantifying fascicles as elementary units of muscle actions. To this end, we employed microCT (microfocus tomography). The short-wavelength and high-energy X-rays equip microCT with the unique advantage of "seeing through" large bodies at high resolution. Combined with novel staining techniques,[12,13] microCT has revolutionized morphological research.[14] We analyzed the trunk of an Asian baby elephant (Figure 1A). As a result of a broken leg, the baby elephant could not be nursed and was euthanized at postnatal day 6. The relatively small size of the baby trunk facilitated our analysis (Figure 1B, upper). To improve the staining of the specimen, we decided to focus on one hemi-trunk and sectioned the trunk parasagittally (Figure 1B, lower). A volume rendering of the hemi-trunk is shown in Figure 1C. This volume image was assembled from a helical trajectory microCT scan with a voxel size of 0.018 mm in the anterior part of the trunk and two circle trajectory microCT scans with a voxel size of 0.025 mm in the posterior part. The microCT scans revealed the elephants' trunk musculature in excellent quality (Figures 1D and 1E). Immediately upon inspection of a transverse cross-section (Figures 1D and 1E), the muscle of the trunk can be separated into many individual compartments, each distinct from one another.

An extremely dexterous part of the elephant trunk is the trunk tip, and we performed a full segmentation of the hemi-trunk tip (Figure 2A). The trunk tip is made up of an immense number of muscle fascicles (3,187 in the hemi-trunk). In the dorsal finger of the elephant trunk, the musculature is made up of remarkable small fascicles (Figure 2B, upper), with muscle fascicles being even smaller than in the ventral lip (Figure 2B, lower). Quantification

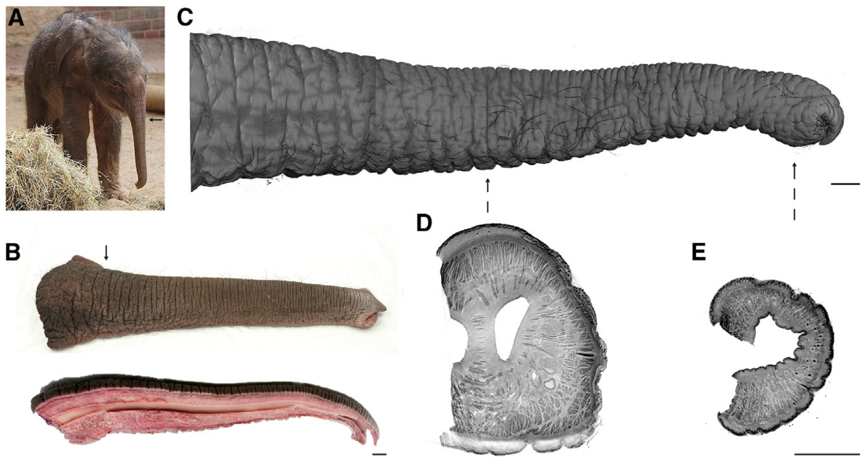

Figure 1. The Asian baby elephant trunk studied here

(A) The Asian elephant calf from which the trunk was dissected (Hoa's baby, picture copyright Zoo Leipzig).

(B) Dorsal view of the complete trunk specimen (upper). The left hemi-trunk before staining, scanning, and analysis (lower). The solid arrow indicates the longitudinal position shown by the arrow in (A). Scale bar in all panels, 1 cm.

(C) Lateral view of the elephant trunk from a volume rendering of the composite microCT scan.

(D) A transverse cross-section through the medial trunk region of the microCT volume. The dashed arrow indicates the longitudinal position in (C).

(E) Same as in (D) for the trunk-tip region.

To facilitate description, we show the left hemi-trunk that we imaged and analyzed mirrored as a right hemi-trunk in this and other figures.

See also Figure S1 for a summary of earlier work on trunk musculature.

shows a smaller mean fascicle length (by 37%) and volume (by 43%) in the dorsal compared to the ventral trunk tip region. The fingertip comes to a tiny point and at the extremity only consists of radial muscle fascicles (Figure 2C). To sort muscles, we applied principal component analysis, which suggested the presence of only two types of muscle fascicles (radial [blue] and longitudinal [yellow]; Figure 2C) in the trunk tip. The quantitative separation of longitudinal and radial muscle types was clear (Figure 2D). Other parts of the trunk tip consist of both longitudinal and radial fascicles, interwoven to form the dense, cross-hatched structure of the muscular hydrostat. The mean volume of dorsal finger fascicles is around 0.01 mm^3, i.e., the elephant trunk finger is made up of truly microscopic muscles (Figure 2E). We also performed conventional muscle histology and prepared hematoxylin and eosin-stained sections from the non-iodine-stained hemi-trunk (Figure S2). This analysis confirmed key results of our X-ray tomography. Specifically, we observed a mesh of larger longitudinal and radial muscle fascicles in the proximal finger and ventral lower trunk-tip lip, compared to much smaller radial muscle fascicles in the distal trunk finger. Our analysis of the trunk tip revealed an extraordinarily filigree muscle mesh.

To understand the muscular architecture of the trunk shaft, we performed dense reconstructions of all fascicles that ran through a coronal section at a mid-level of the trunk (Figure 3). The muscle fascicles of the mid-level trunk shaft were different from the ones encountered in the trunk tip. Specifically, fascicles extended many centimeters around the mid-section (Figure 3A). Altogether, 560 fascicles traversed the hemi-trunk at the middle section (Figure 3B). Shaft-muscle fascicles were structurally diverse (Figure 3C). We visually classified fascicle types colored according to muscle type; in a cross-section of the trunk scan, an orderly tiling of the trunk by different muscle fascicle types was observed (Figure 3D). We slightly displaced fascicles, according to type, to improve visualization in a volume rendering shown in Figure 3E. We visually distinguished three subtypes of radial muscle fascicles. Dorsal radials (dark blue; Figures 3D and 3E) are densely packed, homogeneous, and thick radial fascicles. Lateral radials (medium blue; Figures 3D and 3E) are thinner and variable in insertion point and appearance. Ventral radials (light blue; Figures 3D and 3E) are similar in appearance to, but noticeably fewer than, dorsal ones. We also distinguish three subtypes of longitudinal muscle fascicles. Dorsal longitudinals (yellow; Figures 3D and 3E) are arranged in the periphery of the dorsal trunk and are similar in appearance to (albeit much larger than) longitudinal muscles of the trunk tip. Two types of ventral longitudinal muscles are apparent. The ventral inner obliques (red; Figures 3D and 3E) turn upward, whereas the ventral outer obliques (salmon; Figures 3D and 3E) turn downward. These oblique fascicles are positioned laterally and stacked on top of each other (an arrangement often seen in fascicles of skeletal muscles) and—unlike other elephant trunk muscles—they curve. Finally, there is a small number of transversal muscles (green; Figures 3D and 3E), most of them spanning between the nostrils across the midline. The sheer size of the various longitudinal muscles and curving of the ventral oblique muscles is well visible. Volumes of different muscle types differed significantly (Figure 3F). Shaft muscle fascicles were much larger than trunk-tip fascicles. Figure S3 shows an analysis of the proximal shaft-muscle fascicles based on their dense reconstruction. The muscle architecture of the proximal shaft is similar to the middle shaft. Compared to the middle shaft, the same types of fascicles can be identified proximally; they are slightly larger and fewer (362 fascicles) and traverse a proximal shaft section. There are noticeably more and larger transversal muscles proximally, however. Another interesting difference between the middle and proximal shaft concerns the ratio of dorsal and ventral muscles. The middle shaft contains a three times larger volume of dorsal than ventral radial fascicles. As the contraction of radial fascicles extends a muscular hydrostat like the trunk, we expect the dorsal trunk to be more extendable than the ventral trunk (as reported previously[10]). Similarly, the middle shaft contains a larger fraction of ventral longitudinal fascicles (ventral inner and outer obliques) than dorsal longitudinals, i.e., the middle trunk has more muscle mass for ventral than for dorsal contraction. Both asymmetries give the middle trunk more inward than outward bending force. Such dorsal-ventral asymmetries are not seen in the proximal trunk, where dorsal and ventral radial and longitudinal muscles have similar volume. In summary, the shaft musculature is much coarser than the tip musculature and the middle shaft appears to be specialized for inward bending.

CellPress
OPEN ACCESS

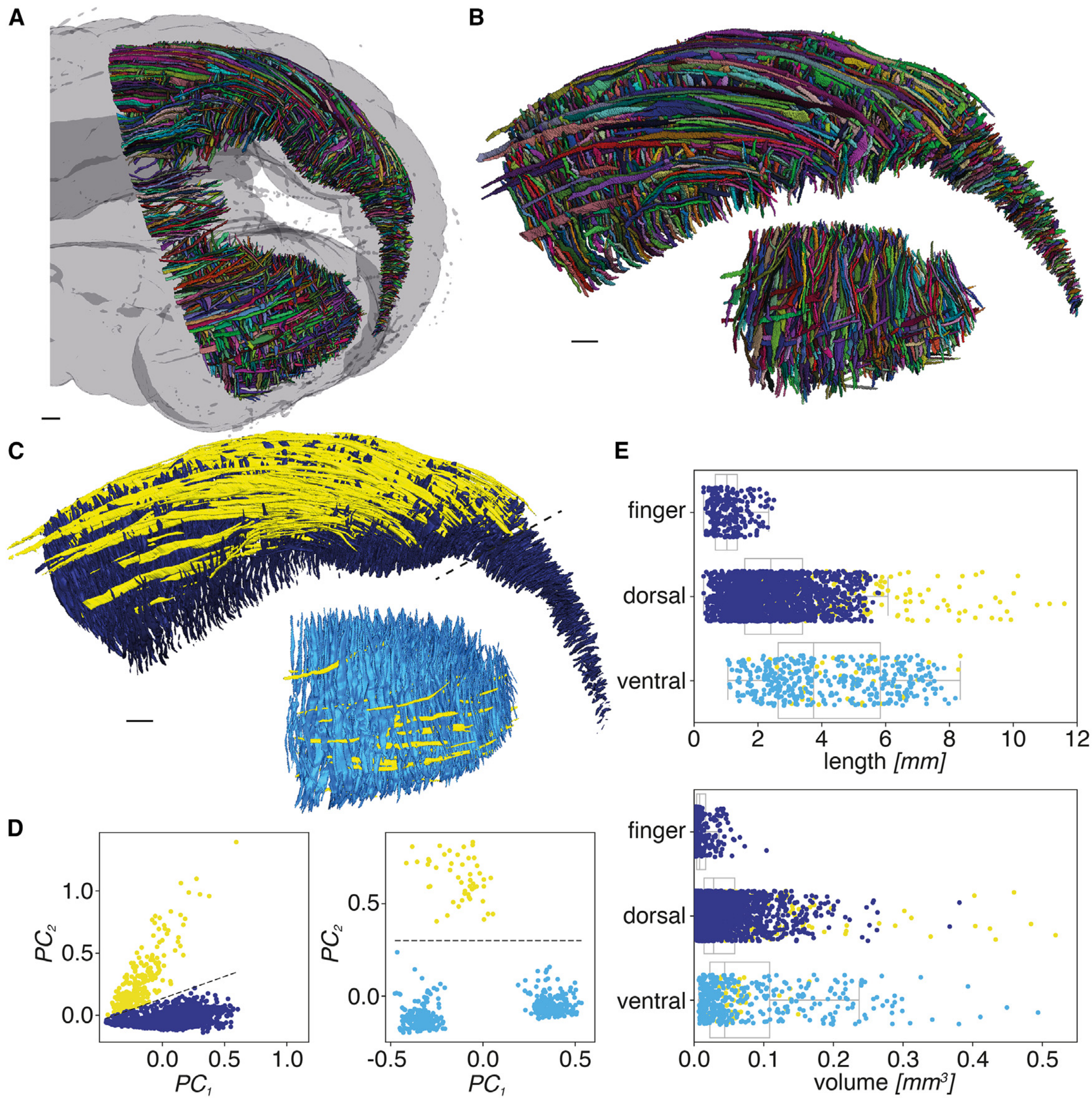

Figure 2. Trunk-tip segmentation reveals very small individual muscle fascicles

(A) All fascicles segmented in the hemi-trunk tip. Scale bar in all panels, 1 mm.

(B) Dorsal trunk finger (upper) and ventral trunk tip (lower) segmentations, slightly displaced for better visualization.

(C) Same as (B), with fascicles colored by longitudinal (yellow), dorsal radial (dark blue), and ventral radial (light blue) muscle types. The dashed line indicates the separation between trunk tip and trunk finger.

(D) The two principal components of the metrics used to classify muscle types in the dorsal (left) and ventral (right) regions. The dashed line indicates the separation between classes. Conventions as in (C).

(E) Length (upper) and volume (lower) metrics of all complete fascicle segmentations in dorsal and ventral trunk tip and trunk finger. Metrics are separated by trunk region. Conventions as in (C).

See also Figure S2 for a comparison of conventional histology and microCT of trunk tip musculature.

A synopsis of trunk muscular architecture is provided in Figure 4. We show volume renderings of fascicles, color-coded according to muscle type, superimposed on a rendering of the entire trunk in Figure 4A; see also Figure S4 for visualization of the orientation of longitudinal and oblique muscles. We show trunk sections with color-coded fascicle types in Figure 4B, which give a sense of the change in muscle architecture across the trunk. There is a marked proximal-to-distal size gradient of fascicles, with proximal fascicles being much larger than distal ones (Figure 4C). As noted earlier, fingertip fascicles, the most distal muscles of the trunk, are indeed extraordinarily small. Comparing the length of fascicles in the index finger of Etruscan shrews, mice, bonobos,[15] humans,[15] and the baby elephant trunk finger (Figure 4D) enforces this idea. While index finger fascicle length increases with animal size and finger length, the trunk finger fascicles of the baby elephant are small beyond expectation and are only slightly longer than in the mouse, an animal that is much smaller. We realize that the elephant trunk finger muscles are not homologous to the other index finger

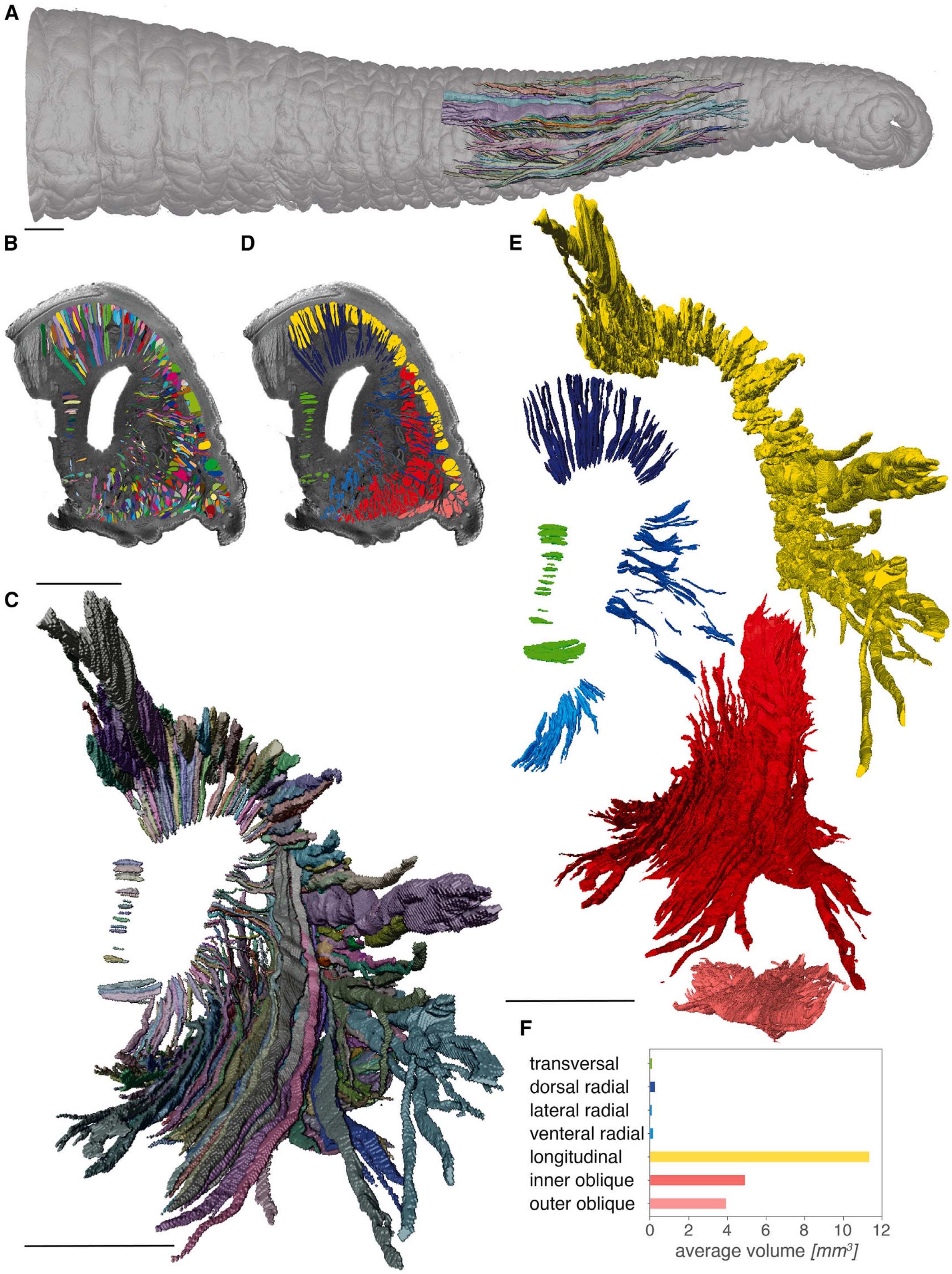

Figure 3. Dense reconstruction of muscle fascicles in the middle of the trunk shaft

(A) Left lateral view of all fascicles segmented in the middle section of the hemi-trunk length. Scale bar in all panels, 1 cm.

(B) Transverse cross-section with muscle fascicle segmentations overlayed for the middle section of the trunk colored by individual fascicles.

(C) Frontal view of segmented muscle fascicles for the middle part colored by individual fascicles.

(D) Transverse cross-section with classified fascicle segmentations overlayed for the middle section of the trunk. Muscles are classified into dorsal longitudinal (yellow), ventral inner oblique (red), ventral outer oblique (salmon), transversal (green), dorsal radial (dark blue), lateral radial (blue), and ventral radial (light blue) fascicles.

(legend continued on next page)

muscles and function in a distinct way (as intrinsic muscles, as opposed to extrinsic muscles in the other mammals), but the size relationship remains noteworthy. Muscle fascicle composition changes across the trunk, an observation confirmed by comparing the volume of fascicle types across different areas of the trunk (Figure 4E). As we noted before, proximal and middle shaft muscles are predominantly longitudinal, whereas the trunk tip and trunk finger are dominated by radial muscles. Across the entire trunk, longitudinal fascicles make up 61% of the musculature, radials make up 32%, and the remaining fraction of fascicles are transversal (Figure 4E). In Figure 4F, fascicle numbers interpolated along the trunk are shown. In terms of number, radial fascicles (in particular, dorsal radials) dominate the trunk. Finally, we extrapolated the complete number of fascicles (Figure 4G) and arrived at an estimate of about 90,000 fascicles, about 85% of which are radials and only 5% of which are longitudinals. We conclude that the elephant trunk contains an incredible number of fascicles and the trunk's distal musculature, which mediates dexterous prehension, is made up of numerous extremely small radial fascicles.

The structure of trunk musculature

Our results align well with previous descriptions of trunk musculature. In particular, many of our muscle reconstructions match with the beautiful drawings provided by Boas and Paulli.[16] Much like Cuvier[3] and later Shoshani,[4] we find that the elephant trunk contains numerous muscle fascicles. Their groundbreaking early anatomical work[3,4] was based on conclusions drawn from the acute dissection of elephant trunks. When it comes to specific numbers (i.e., 30–40,000 Cuvier[3]; 150,000 Shoshani[4]), we think our estimate of 90,000 muscle fascicles has a much firmer footing than earlier work because our estimate is based on partial dense reconstructions rather than on mere extrapolation from cross-sections. Dense reconstructions of muscle fascicles are much more laborious than acute dissections (several years compared to several days of work), but they provide more detail. Specifically, our dense reconstruction indicated that, indeed, each radial muscle fascicle inserts independently, which suggests that thousands of potentially independent actuators operate in the elephant trunk. Our observations on muscle architecture match with the work of Endo et al.[8] Ultimately, total muscle fascicle number will be precisely determined by complete segmentation and reconstruction of several African and Asian elephant trunks. The complex motor plan matches with the massive sensory tactile innervation[17] and complex peripheral sensory specializations[18,19] of the elephant trunk. An important limitation of our work is that it refers to only a single newborn elephant. Unquestionably, further work is required to obtain a more general picture of trunk musculature that also includes adult elephants.

Muscle architecture of the elephant trunk

More important than the number is the muscle architecture revealed by our work. Perhaps the most unexpected feature is the microscopic size of trunk-tip and trunk-finger muscle fascicles. We owe this insight to the excellent resolution of our microCT analysis. Unexpectedly, elephants operate with muscle fascicles much smaller than finger muscles of other mammals. The shaft musculature has a clear lateral symmetry. The idea of radially symmetric trunk action[9] is a misleading impression from the roundish outer trunk, its immense flexibility, and trunk cross-sections, which only poorly reveal muscular organization. In particular, the ventral outer obliques are confined to a ventrolateral trunk position and lack a radial architecture.

Comparison to the octopus

As a muscular hydrostat the octopus arm follows the same confines as those of the elephant trunk. The octopus arm shares longitudinal, oblique, and transversal muscles with the trunk, but lacks radial musculature. Instead, circumferential muscles surround the octopus arm.[20] In addition, the octopus has intrinsic musculature of its suckers and musculature connecting the suckers to its arm shaft.[20] Longitudinal muscle makes up ~60% of the cross-sectional area of the intrinsic muscles in the octopus arm, while transversal and oblique muscle make up ~20% each.[21]

Trunk muscles and trunk movement

It is generally agreed upon that the trunk acts as a muscular hydrostat. Our analysis of trunk muscle structure fleshes out how the muscular hydrostat is structured in the elephant trunk. Recent work investigated how trunk movements might arise from trunk muscles.[11] Using a variety of videographic techniques and cinematic analysis, the authors concluded that trunk movements make use of only a small fraction of "possible" trunk movements.

Miniaturized radial fascicles mediate prehension and trunk-tip fine control

The trunk tip has an extraordinary capacity for prehension and molding according to grasping requirements.[22] Our work shows that such prehension is mediated by a predominantly radial musculature. Our data also emphasize how filigree trunk-tip muscles are, and we assume that the need for fine-grained control of trunk-finger movements drove this evolutionary development. We also think that further analysis of trunk-finger movements will provide insights into the role of different trunk-muscle types. Specifically, we show that the fingertip is made up exclusively of radial muscles. Thus, fingertip movements are mediated by a monotypic musculature, and motor differences between the fingertip and the proximal finger may elucidate how longitudinal muscles add to the motor repertoire. How can the fingertip operate if it contains only radial muscles, whose contraction presumably mediates only finger extension, i.e., where is antagonism that mediates normal muscle action? We think that fingertip radial muscles might act against elastic forces that bend the finger inward and tendons of longitudinal muscles extrinsic to the fingertip might mediate finger bending.

Specialization of the middle trunk for inward bending

The larger fraction of dorsal over ventral radial muscle fascicles in the middle trunk should lead to a larger ability of the dorsal trunk to

(E) Frontal view of classified muscle fascicles (slightly displaced according to fascicle types). Conventions as in (D).

(F) Average volume of different fascicle types in the middle part of the trunk. According to an ANOVA, the volumes were significantly different from one another (test statistic, F 12.6367; $p < 0.0001$).

See also Figure S3 for a dense reconstruction of muscle fascicles for the proximal part of the trunk shaft.

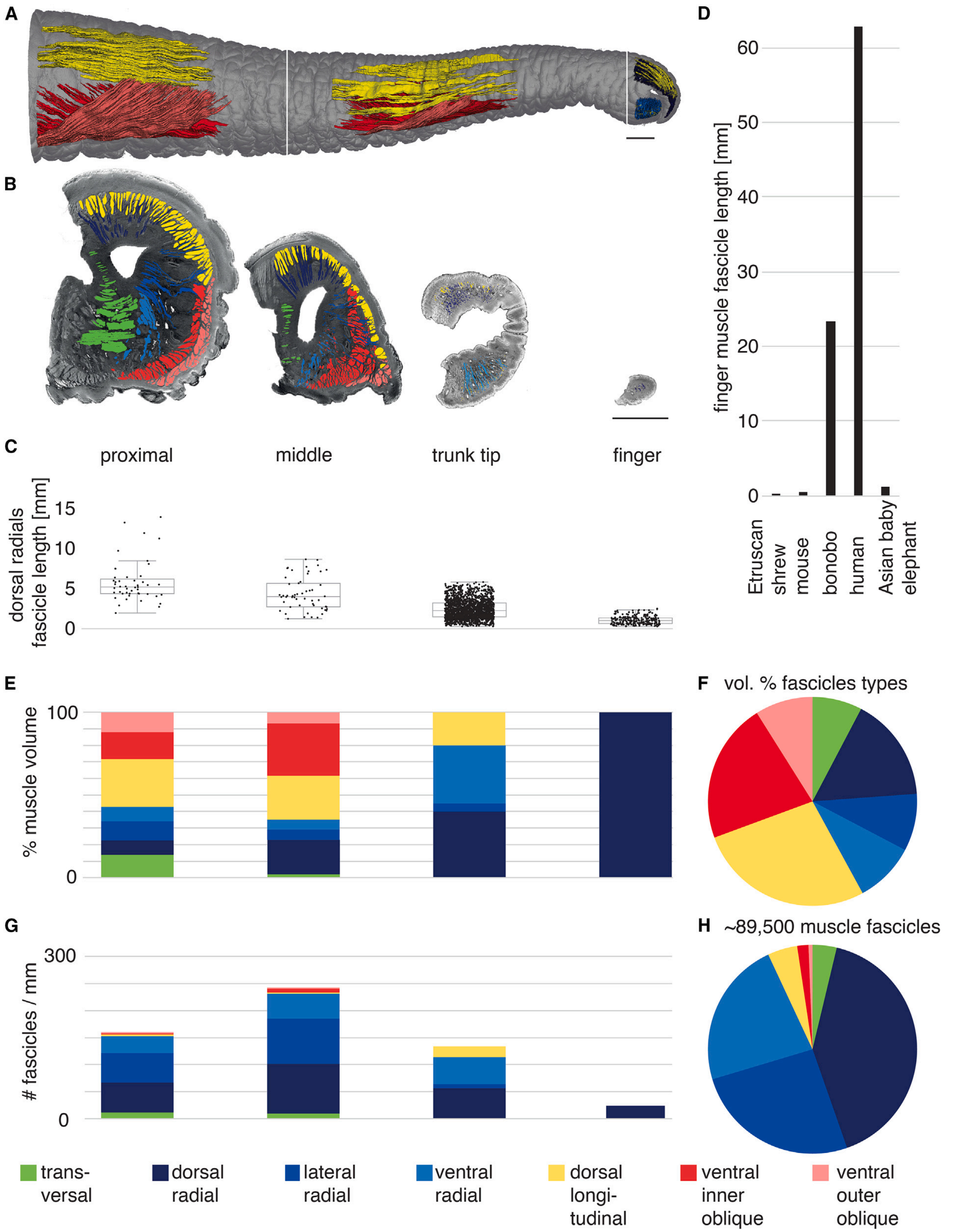

(legend on next page)

extend. Such dorsoventral extension asymmetries were recently observed in African elephants.[10] Similarly, we observed more ventral longitudinal muscle fascicles (upward and downward obliques) than dorsal (parallel) longitudinal muscle fascicles. This dorsoventral asymmetry should lead to a greater ability of the ventral trunk to contract.

Trunk versus hand control

Elephant trunk movements are among the most skillful, rivaled only by primate hand movements. A continuum model, or model describing the mechanical behavior of materials as a continuous mass, has been formulated for the elephant trunk's muscle-tendon system.[9] The trunk's dexterity stems from a combination of size and distribution of the trunk's tendons and muscle masses. Mechanical behavior of the elephant's trunk is similar to other hydrostats, such as squid tentacles and vertebrate tongues. Contraction of radial muscles leads to extension of the trunk, contraction of oblique muscles leads to torsion around the longitudinal axis, and a combination of contracting longitudinal muscles on one side with the radial muscles leads to bending toward that particular side.

To understand trunk motor control, one also needs to consider the brain structures involved. The elephant brain stands out by its very large and complex cerebellum,[23] and the sheer size of this structure points to sophisticated motor control in elephants. Another important aspect is the motoneuronal innervation of the trunk. According to Kaufmann et al.[24] there are about 54,000 neurons in the facial nucleus, and even if all these motor neurons would innervate the trunk, the 2 × 54,000 neurons would barely outnumber the 90,000 muscle fascicles of the trunk. Based on a number of assumptions, Kaufmann et al.[24] suggested that the dorsal and lateral subnuclei represent the dorsal and ventral sections of the trunk, respectively, and in this case only an estimated 40,000 motor neurons innervate the entire Asian elephant trunk. According to these numbers, there is not a massive convergence of motor neurons on elephant trunk muscle fascicles. The innervation patterns of the human hand musculature are very different from that, and more than a thousand motor neurons[25] innervate about 30 hand muscles. We therefore wonder if primate hand control is regulated via the fine control of muscle contraction strength, whereas the elephant exerts trunk control via the number of recruited muscle fascicles. The evolution of such different motor strategies for prehension (fine control of few large actuators, as in the primate hand, versus the emergence of thousands of small actuators in the elephant trunk) is noteworthy. By itself, understanding the complex structure of the elephant trunk provides insight into an amazing muscle system, and we think it would be worthwhile to explore the relevance of these findings to soft robotics applications.[26,27]

Conclusion

The musculature of the elephant trunk is one of a kind. The segmentation of this musculature reveals unexpected filigree and complex architecture, paving a way toward describing the dexterous trunk movements in terms of the actions of the constituting muscular elements.

STAR★METHODS

Detailed methods are provided in the online version of this paper and include the following:

- KEY RESOURCES TABLE
- RESOURCE AVAILABILITY
  - Lead contact
  - Materials availability
  - Data and code availability
- EXPERIMENTAL MODEL AND SUBJECT DETAILS
  - Asian elephant, Elephas maximus
  - Specimen condition
- METHOD DETAILS
  - Elephant trunk preparation and staining
  - Conventional histology of trunk tissue
  - Trunk microCT scanning and preprocessing
  - Trunk muscle fascicle segmentation
  - Individual muscle fascicle analysis
  - Muscle type classification
  - Trunk tip muscle type
- QUANTIFICATION AND STATISTICAL ANALYSIS
  - Muscle number extrapolation
  - Statistical analyses

SUPPLEMENTAL INFORMATION

Supplemental information can be found online at https://doi.org/10.1016/j.cub.2023.09.007.

ACKNOWLEDGMENTS

We thank Andreea Neukircher for comments on the manuscript. We thank Léo Botton-Divet and Undine Schneeweiß for technical assistance. Supported by the Bernstein Center for Computational Neuroscience (BCCN) Berlin, Humboldt-Universität zu Berlin, and NeuroCure Cluster of Excellence (Exc 2049-390688087).

Figure 4. Muscle size, fascicle types, and fascicle number across the whole trunk

(A) Lateral view of all fascicles segmented in the hemi-trunk length. Scale bar, 1 cm.
(B) Transverse cross-sections with classified fascicle segmentations overlayed for the proximal, middle, and tip section of the trunk. Muscle fascicle classification follows the legend at the bottom of the figure. Scale bar, 1 cm.
(C) Length of dorsal radial fascicles in proximal, middle, trunk-tip, and trunk-finger sections.
(D) Comparison of the length of index finger muscle fascicles between Etruscan shrew, mouse, bonobo, human, and finger muscle fascicle length in the Asian baby elephant. Data of bonobos and humans come from Van Leeuwen et al.[15]; Etruscan shrew and mouse finger fascicles were segmented by us.
(E) Muscle volume fraction of different fascicle types in proximal, middle, trunk-tip, and trunk-finger sections from left to right.
(F) Muscle volume fraction of different fascicle types across the entire trunk.
(G) Muscle fascicle number per mm of different fascicle types in proximal, middle, trunk-tip, and trunk-finger sections from left to right.
(H) Muscle fascicle number of different fascicle types across the entire trunk.
See also Figure S4 for a visualization of proximal longitudinal and oblique muscle fascicles.

AUTHOR CONTRIBUTIONS

Conceptualization, L.L.L., L.E., and M.B.; methodology, L.L.L., L.E., A.S., O.L., D.B., J.A.N., T.H., and M.B.; investigation, L.L.L., L.E., A.S., O.L., and M.B.; formal analysis, L.L.L., L.E., and M.B.; writing, L.L.L., L.E., A.S., O.L., D.B., J.A.N., T.H., and M.B.; supervision, M.B.; funding acquisition, M.B.

DECLARATION OF INTERESTS

The authors declare no competing interests.

INCLUSION AND DIVERSITY

We support inclusive, diverse, and equitable conduct of research.

Received: July 8, 2023
Revised: August 15, 2023
Accepted: September 1, 2023
Published: September 26, 2023

REFERENCES

1. Kier, W.M., and Smith, K.K. (1985). Tongues, tentacles and trunks: the biomechanics of movement in muscular-hydrostats. Zool. J. Linn. Soc. *83*, 307–324.
2. Smith, K.K., and Kier, W.M. (1989). Trunks, tongues, and tentacles: moving with skeletons of muscle. Am. Sci. *77*, 28–35.
3. Cuvier, G., and MacGillivray, W. (1839). The Animal kingdom of the Baron Cuvier. J. Nat. Hist. *31*.
4. Shoshani, J. (1997). It's a nose! It's a hand! It's an elephant's trunk! Nat. Hist. *106*, 36–45.
5. Hooper, S., and Schulz, A. (2020). Proboscidea morphology. In Encyclopedia of Animal Cognition and Behavior (Springer International Publishing), pp. 5660–5665. https://doi.org/10.1007/978-3-319-47829-6_1320-1.
6. Shoshani, J. (1982). On the dissection of a female Asian elephant (*Elephas maximus maximus* Linnaeus, 1758) and data from other elephants. Elephant *2*, 3–93. https://doi.org/10.22237/elephant/1521731887.
7. Wilson, J.F., Mahajan, U., Wainwright, S.A., and Croner, L.J. (1991). A continuum model of elephant trunks. J. Biomech. Eng. *113*, 79–84. https://doi.org/10.1115/1.2894088.
8. Endo, H., Hayashi, Y., Komiya, T., Narushima, E., and Sasaki, M. (2001). Muscle architecture of the elongated nose in the Asian elephant (Elephas maximus). J. Vet. Med. Sci. *63*, 533–537.
9. Wilson, J.F. (1985). Compliant Robotic Structures (Department of Civil and Environmental Engineering, Duke University).
10. Schulz, A.K., Boyle, M., Boyle, C., Sordilla, S., Rincon, C., Hooper, S., Aubuchon, C., Reidenberg, J.S., Higgins, C., and Hu, D.L. (2022). Skin wrinkles and folds enable asymmetric stretch in the elephant trunk. Proc. Natl. Acad. Sci. USA *119*, e2122563119.
11. Dagenais, P., Hensman, S., Haechler, V., and Milinkovitch, M.C. (2021). Elephants evolved strategies reducing the biomechanical complexity of their trunk. Curr. Biol. *31*, 4727–4737.e4. https://doi.org/10.1016/j.cub.2021.08.029.
12. Metscher, B.D. (2009). MicroCT for comparative morphology: simple staining methods allow high-contrast 3D imaging of diverse non-mineralized animal tissues. BMC Physiol. *9*, 11.
13. Metscher, B.D. (2009). MicroCT for developmental biology: a versatile tool for high-contrast 3D imaging at histological resolutions. Dev. Dyn. *238*, 632–640.
14. Cunningham, J.A., Rahman, I.A., Lautenschlager, S., Rayfield, E.J., and Donoghue, P.C.J. (2014). A virtual world of paleontology. Trends Ecol. Evol. *29*, 347–357.
15. Van Leeuwen, T., Vanhoof, M.J.M., Kerkhof, F.D., Stevens, J.M.G., and Vereecke, E.E. (2018). Insights into the musculature of the bonobo hand. J. Anat. *233*, 328–340.
16. Boas, J.E.V., and Paulli, S. (1908). The Elephant's Head: Studies in the Comparative Anatomy of the Organs of the Head of the Indian Elephant and Other Mammals (Carlsberg-Fund).
17. Purkart, L., Tuff, J.M., Shah, M., Kaufmann, L.V., Altringer, C., Maier, E., Schneeweiß, U., Tunckol, E., Eigen, L., Holtze, S., et al. (2022). Trigeminal ganglion and sensory nerves suggest tactile specialization of elephants. Curr. Biol. *32*, 904–910.e3.
18. Rasmussen, L.E., and Munger, B.L. (1996). The sensorineural specializations of the trunk tip (finger) of the Asian elephant, *Elephas maximus*. Anat. Rec. *246*, 127–134.
19. Deiringer, N., Schneeweiß, U., Kaufmann, L.V., Eigen, L., Speissegger, C., Gerhardt, B., Holtze, S., Fritsch, G., Göritz, F., Becker, R., et al. (2023). The functional anatomy of elephant trunk whiskers. Commun. Biol. *6*, 591.
20. Kier, W.M. (2016). The musculature of coleoid cephalopod arms and tentacles. Front. Cell Dev. Biol. *4*, 10.
21. Kier, W.M., and Stella, M.P. (2007). The arrangement and function of octopus arm musculature and connective tissue. J. Morphol. *268*, 831–843.
22. Schulz, A.K., Reidenberg, J.S., Ning Wu, J., Ying Tang, C., Seleb, B., Mancebo, J., Elgart, N., and Hu, D.L. (2023). Elephant trunks use an adaptable prehensile grip. Bioinspir. Biomim. *18*, 026008.
23. Maseko, B.C., Spocter, M.A., Haagensen, M., and Manger, P.R. (2012). Elephants have relatively the largest cerebellum size of mammals. Anat. Rec. *295*, 661–672.
24. Kaufmann, L.V., Schneeweiß, U., Maier, E., Hildebrandt, T., and Brecht, M. (2022). Elephant facial motor control. Sci. Adv. *8*, eabq2789.
25. Gesslbauer, B., Hruby, L.A., Roche, A.D., Farina, D., Blumer, R., and Aszmann, O.C. (2017). Axonal components of nerves innervating the human arm. Ann. Neurol. *82*, 396–408.
26. Neppalli, S., Jones, B., McMahan, W., Chitrakaran, V., Walker, I., Pritts, M., Csencsits, M., Rahn, C., and Grissom, M. (2007). Octarm-a soft robotic manipulator. In IEEE/RSJ International Conference on Intelligent Robots and Systems, p. 2569.
27. Guan, Q., Sun, J., Liu, Y., Wereley, N.M., and Leng, J. (2020). Novel bending and helical extensile/contractile pneumatic artificial muscles inspired by elephant trunk. Soft Robot. *7*, 597–614.

CellPress
OPEN ACCESS

STAR★METHODS

KEY RESOURCES TABLE

REAGENT or RESOURCE	SOURCE	IDENTIFIER
Biological samples		
Elephant specimen	IZW as specified in this paper	N/A
Chemicals, peptides, and recombinant proteins		
Iodine-Potassium Iodide (Lugol's Solution)	Morphisto	Cat. # 10255
Hematoxylin and eosin solution (H&E stain)	Sigma-Aldrich	Cat. # HT110232-1L
Deposited data		
Raw and analyzed data	This paper; German Neuroinformatics Node	https://gin.g-node.org/elephant/muscle
Software and algorithms		
Amira ZIB Edition 2021, 2022, 2023	Zuse Institute Berlin	Thermo Scientific Amira - Imaging Data & Processing; RRID: SCR_007353
Python versions 3.6+	Python Software Foundation	https://www.python.org
Excel	Microsoft	https://www.microsoft.com/excel
Other		
YXLON FF20 CT scanner	YXLON International GmbH, Hamburg, Germany	https://yxlon.comet.tech/en/products/ff20-ct; RRID: SCR_020903
Neurolucida system	Microbrightfield	https://www.mbfbioscience.com/products/neurolucida; RRID: SCR_001775

RESOURCE AVAILABILITY

Lead contact

Further information and requests for resources and reagents should be directed to and will be fulfilled by the lead contact, Michael Brecht (michael.brecht@bccn-berlin.de).

Materials availability

This study did not generate new unique agents.

Data and code availability

- Muscle fascicle data have been deposited at the German Neuroinformatics Node and are publicly available as of the date of publication. The link is listed in the key resources table.
- This paper does not report any original code.
- Any additional information required to reanalyze the data reported in this paper is available from the lead contact upon request.

EXPERIMENTAL MODEL AND SUBJECT DETAILS

The elephant specimen used for analysis came from a zoo elephant collected by the IZW (Leibniz Institute for Zoo and Wildlife Research, Berlin) in agreement with CITES regulations. The animal included in the study was euthanized by experienced zoo veterinarians due to insurmountable health complications.

Asian elephant, Elephas maximus

Data obtained from a newborn female Asian elephant was used for the study. The elephant was birthed by the Asian elephant cow Hoa in Leipzig, Germany and was six days old upon death. The trunk did not appear to be affected by the health situation of the individual.

Specimen condition

The elephant trunk specimen arrived frozen.

METHOD DETAILS

Elephant trunk preparation and staining

Trunk preparation

The elephant trunk was cut in half longitudinally along the dorsal to ventral line of symmetry. The left half of the trunk, relative to the specimen, was used for data collection in the present study.

Trunk staining

The trunk was allowed to thaw for a day and then placed into Lugol's iodine solution (Cat. #10255) at 1% concentration. To follow staining progress, weekly microCT scans were made with the solution being replaced after each scan. Sufficient staining was achieved at a time of 33 days, at which point the trunk was placed into Lugol's iodine solution at 0.5% concentration.

Conventional histology of trunk tissue

Iodine-staining is incompatible with subsequent histology. We therefore prepared sections from the unstained hemi-trunk for conventional muscle histology. After fixation in 4% paraformaldehyde solution for several weeks, we cut 3 mm thick sections from the medial parts of the trunk finger and the lower lip of the trunk tip and placed them in 30% sucrose solution for 2 days. Then we cut thin (60 μm) sections on a cryostat and stained them with hematoxylin and eosin solution (Cat. #HT110232-1L). Sections were cover-slipped and micrographs were taken on a Neurolucida system (Microbrightfield, Willistion, USA).

Trunk microCT scanning and preprocessing

MicroCT scans were performed with a YXLON FF20 CT system (YXLON International GmbH, Hamburg, Germany) equipped with a PerkinElmer Y Panel 4343 CT detector and 190 kV nano focus transmission tube. An anterior section of the trunk, measuring 13 cm, was scanned by helical trajectory microCT after 33 days of staining. Medial and proximal sections of the trunk, measuring an additional 10 cm total, were scanned in two parts by circle trajectory microCT after an additional 84 days of the lower concentration stain. Before segmentation, the anterior image was preprocessed by Adaptive Histogram Equalization in the Amira software (AmiraZIBEdition 2021, 2022, and 2023, Zuse Institute Berlin) for better image contrast. The medial and proximal images were analyzed without preprocessing.

Trunk muscle fascicle segmentation

Labeling of individual muscle fascicles was obtained by manual segmentation in the Amira software. To do so, a combination of the 'Lasso' and 'Brush' modules in Amira together with the 'Interpolation' tool were predominantly used. The total time required to manually segment all fascicles was approximately 3,000 h. As the total number of fascicles in the entire trunk is huge, points along the longitudinal length of the trunk were chosen and transverse sections were segmented in their entirety. These include a complete reconstruction of the initial 1.5 cm of the tip, a medial section at 8.7 cm from the tip, and a proximal section at 18.6 cm from the tip. Partitions with a longitudinal length of 5.4 cm, centered on the medial and proximal sections, were used for analysis. The total length of the trunk image was 21.6 cm. At the medial and proximal sections, all muscles passing through the chosen transverse planes were segmented fully, encompassing any branching of individual fascicles. For comparison of muscle fascicle length in different mammals, we also segmented 50 fascicles of the IOD (musculus interossei dorsalis) for both the Etruscan shrew and the mouse.

Individual muscle fascicle analysis

The properties of each muscle fascicle were analyzed using the 'Label Analysis' module in Amira. Primary metrics included length and volume. Secondary metrics included orientation angles. The distance transform of the trunk's muscle region, obtained by manual segmentation, was used in addition. Even though our microCT scan contained most of the baby elephant trunk, some muscle fascicles could not be completely reconstructed, because they left the image volume. This problem affected only a small part of a small subset of longitudinal muscle fascicles, mainly in the proximal shaft reconstruction section. We did not correct for this problem in our muscle number extrapolation, which should lead to a slight underestimate of the size of longitudinal muscles and hence, a slight overestimate of longitudinal muscle fascicle number.

Muscle type classification

Using the quantitative muscle fascicle metrics, each fascicle can be categorized as part of a functionally defined muscle mass. Thoroughly described in previous literature, the muscular hydrostat represented by the elephant trunk consists of three fundamental types of muscles: longitudinal, radial, and transversal.

Trunk tip muscle type

In the trunk tip, separate classifications of the dorsal and ventral fascicles were performed. For both regions, principal component analysis (PCA) was used to reduce the dimensionality of the metrics to two principal components. Then, classification was performed manually by linear separation of visibly distinct classes. In the dorsal region, the metrics used were length, volume, range of distance transform values, and range of distances from the furthest anterior point on the trunk. Each range was determined by considering all voxels within a fascicle. In the ventral region, metrics were solely the two orientation angles of the length calculation. PCA and plotting were performed using Python (Python Software Foundation).

In the middle and proximal sections, manual classification of trunk fascicles was performed. Using the 'Label Region Classifier' module in Amira, each fascicle was added to their respective class.

QUANTIFICATION AND STATISTICAL ANALYSIS

Muscle number extrapolation

From the three completely segmented sections of the trunk musculature (i.e., tip, middle, and proximal), a prediction of the total fascicle number was made. Description of how the muscle fascicle number was estimated in four distinct trunk regions is provided below.

Trunk-tip region

The hemi-trunk tip region was fully reconstructed (see Figure 2) and contained 3,187 muscle fascicles. We classified muscle fascicle types as documented in Figure 2.

Tip-to-shaft transition

We visually inspected the muscle architecture of the region posterior to the trunk-tip and found that muscle fascicle patterns gradually change from the trunk tip-like organization to a trunk shaft-like organization, as we had observed in the middle trunk section. At 5 mm posterior to our reconstruction, the nasal septum appeared and fascicles looked more shaft-like. Accordingly, we assumed that the tip-shaft transitional region, from the end of the trunk-tip reconstruction to the nasal septum, to have the same fascicle number and organization as the posterior of our trunk-tip reconstruction. In the 5 posterior millimeters of our trunk-tip reconstruction, we observed 1,050 fascicles per hemi-tip, the number of fascicles thus assumed to be in the tip-shaft transitional hemi-region. Fascicle types are assumed to be in equal proportions as well.

Middle-shaft region

We extrapolated fascicle numbers in the middle-shaft region according to the dense reconstruction of fascicles in the middle trunk section (see Figure 3). We first constructed and cross-checked all fascicles passing transversely through one middle section of the trunk. To make our extrapolation robust, we then extended the dense reconstruction to 14 (18 μm) sections, i.e., 252 μm of trunk. For each fascicle type, we computed the volume contained in the 252 μm section and divided it by the average volume of the respective fascicle type from the dense reconstruction. Thus, we obtained the number of fascicles of a particular type in the 252 μm volume. From the number of fascicles contained in this volume, we extrapolated middle-trunk fascicles beginning distally 5 mm behind the dense trunk tip reconstruction to (proximally) a point between the middle and proximal dense reconstructions. This region spanned 114.47 mm and contained 30,364 fascicles in the hemi-middle region. From our visual inspection of the muscle architecture, we expect that this estimate slightly overestimates fascicle numbers on the proximal side and slightly underestimates fascicle numbers on the distal side of the dense reconstruction.

Proximal-shaft region

We extrapolated fascicle numbers in the proximal-shaft region as outlined above for the middle-shaft region from the dense reconstruction of fascicles in the trunk proximal section (see Figure S2). We first constructed and cross-checked all fascicles passing through one proximal section of the trunk. To make our extrapolation more robust, we then extended the dense reconstruction to 10 (25 μm) sections, i.e., 250 μm of trunk. From the numbers of fascicles contained in this volume, we extrapolated proximal trunk fascicles in the proximal third of the trunk. This region spanned 79.53 mm and contained 15,041 fascicles in the hemi-proximal region. As noted for the middle section, we expected that this proximal estimate slightly overestimates fascicle numbers on the proximal side and slightly underestimates fascicle numbers on the distal side of the dense reconstruction.

In sum of the four regions, we estimate a total of 44,732 fascicles in the hemi-trunk, and hence, 89,465 fascicles in the entire trunk.

Statistical analyses

Statistical analyses and plotting were performed using Excel (Microsoft) and in Figures 3F and S3F we used the two-way ANOVA Calculator tool from the online Social Science Statistics webpage (https://www.socscistatistics.com).